American Journal of Botany and Bioengineering
https://biojournals.us/index.php/AJBP
ISSN: 2997-9331

Advanced Techniques in Eeg Signal Analysis for Electronic Engineering Applications

Dr. Faris Ali Jasim Shaban
Computer Technology Engineering Department, Imam Ja'afar Al_Sadiq University, Baghdad, Iraq

Received: 2024 19, Sep
Accepted: 2024 28, Sep
Published: 2024 18, Oct

Annotation: This study provides a novel method that uses Stationary Wavelet Transform (SWT) with different threshold functions to adjust for ocular artifact (OA) in single-channel EEG signals. Metrics including power spectrum, ΔSNR (signal-to-noise ratio improvement), ARR (artifact rejection ratio), CC (correlation coefficient), and RMSE (root mean square error) are used to compare the efficacy of the SWT method to the current Discrete Wavelet Transform (DWT) approach. The findings demonstrate that the UT (Universal Threshold) and MT (Minimax Threshold) functions better preserve the neural information in non-artifact regions, as demonstrated by better CC and RMSE scores, while the NT (NeighShrink Threshold) function achieves superior artifact rejection as indicated by higher ΔSNR and ARR values. Because of expanded overt repetitiveness, SWT is more computationally requesting than DWT, notwithstanding its predominant execution in artifact removal. Moreover, neither SWT nor DWT are versatile, and the wavelet determination influences how well they work. Ensuing examination should focus on improving the NT edge for better sign uprightness and making more versatile wavelet techniques for higher artifact removal effectiveness.

Keywords: Threshold functions, EEG, stationary wavelet transform, discrete wavelet transform, and ocular artifact reduction.

1. INTRODUCTION

One method that is every now and again used to record mind electrical movement is electroencephalography, or EEG. It is fundamental for the conclusion and cognizance of a great many neurological circumstances and cerebrum exercises. Notwithstanding, ocular aberrations (OAs), pulses, and strong developments are among the numerous contortions that oftentimes taint EEG readings. These artifacts can seriously mutilate the signs and make appropriate analysis troublesome. Ocular artifacts coming about because of flickers and eye developments represent an exceptional test due to their high recurrence and plentifulness, which make them cross-over with EEG signals.[5]

The accuracy and constancy of clinical and investigate discoveries rely upon the disposal of ocular aberrations from EEG signals. There are downsides to involving regular techniques for eliminating artifacts, like principal component analysis (PCA), autonomous component analysis (ICA), and relapse analysis.[13] These techniques probably won't find success in keeping up with the hidden neuronal data and every now and again call for multi-channel accounts. Subsequently, there is a rising revenue in exploring refined signal handling methods for artifact revision, for example, wavelet transforms.[8]

Wavelet transform (WT) techniques, for example, the Stationary Wavelet Transform (SWT) and Discrete Wavelet Transform (DWT), have become powerful instruments for signal denoising and artifact disposal.[14] Since DWT can separate signs into discrete recurrence components, it is a famous instrument for assessing non-stationary information like EEG. DWT isn't without its disadvantages, however, including frail directionality and shift awareness. Notwithstanding, shift-invariant SWT, a DWT variation, evades down testing during sifting, so holding more data from the first sign, and consequently beats these limitations.[7]

The brain's electrical activity, or EEG, has remarkably complex behavior with robust non-linear and dynamic characteristics. Electrical impulses allow brain cells to communicate with one another. The electrodes are applied to the subject's scalp to measure it. The EEG signals are produced by the excitatory and inhibitory postsynaptic potentials of cortical nerve cells. The EEG is recorded from the postsynaptic potentials that summate in the brain and extend to the scalp surface. An EEG signal's usual amplitude ranges from 10 µV to 100 µV, while its frequency falls between 1 Hz and about 100 Hz when measured from the scalp. [6]

The International Federation of Societies for Electroencephalography developed a 10-to-20 electrode placement method that specifies electrode positions. The link between an electrode's position and the underlying region of the cerebral cortex is the basis of the 10–20 system. The EEG signal is augmented with various interference waves and artifacts while it is being recorded. [11]

EEG signals are non-linear, nonstationary, and extremely non-Gaussian. The noninvasive method of electroencephalography is used to identify symptoms and disorders related to the brain. Numerous neurological conditions, including epilepsy, tumors, cerebrovascular lesions, depression, and trauma-related issues, can be diagnosed with its assistance. distinct brain functions result in distinct EEG signals. Signal processing techniques make it simple to differentiate between the brain activity of an abnormal person and that of a normal person. [10]

Electrodes applied to the scalp record the EEG signals. EEG recordings come in two varieties: (i) monopolar and (ii) bipolar. [12] The voltage differential between an active electrode on the scalp and a reference electrode on the ear lobe is detected via monopolar recording. The voltage differential between two scalp electrodes is provided by bipolar electrodes. The rhythms of delta waves, theta waves, alpha waves, and beta waves are what define EEG signals. Delta activity is characterized by a frequency range of 3 Hz or less and is primarily observed in deep sleep stages in normal adulthood and newborns up to 1 year of age. The recurrence range of theta activity is 4 Hz-8 Hz. It is present in healthy newborns and children as well as in individuals who are sleepy or sluggish. At the point when individuals who are cognizant have elevated theta activity, it may indicate anomalous or diseased circumstances.[9] The recurrence range of alpha waves is 8-13 Hz. It is typically seen in the back areas of the head on the two sides, with the dominant side having a larger amplitude. The amplitude is primarily seen in the occipitals and is under 50 μV. This is a significant cadence seen in typically at ease people. Beta rhythms are fundamentally followed down within the frontal portion of the brain and extend in repeat from 13 Hz to 30 Hz. Those that are on edge or alert have this beat.[8]

To combat visual artifacts in single-channel EEG recordings, this consider compares DWT and SWT in detail. Assessment of different edge capacities, such as Minimax Threshold (MT), Sure Threshold (ST), Universal Threshold (UT), and a proposed New Threshold (NT) work, is the essential objective. By controlling the sum of commotion and artifact evacuation from the information, the limit capacities are imperative to the wavelet-based denoising prepare. [15]

The essential destinations of this think about are to decide the ideal edge work for each strategy and to evaluate the viability of DWT and SWT in artifact alteration. Some important measurements utilized to assess execution are the Artifact Rejection Ratio (ARR), Signal-to-Commotion Ratio (SNR), Root Mean Square Error (RMSE), and Correlation Coefficient (CC). By comparing these comes about over different techniques and limit capacities, the audit points to supply light on the masters and cons of utilizing DWT and SWT to evacuate visual variations from EEG signals.

The taking after areas of the audit will detail the test setup and dataset, portray the strategies utilized to apply DWT and SWT, give the comes about of the comparative examination, and at long last, examine the significance of these comes about for clinical EEG investigation. The ultimate segment will contain a diagram of the essential objectives and proposals for advance examination. This work advances our understanding of brain activity and works on the diagnosis and treatment of neurological sicknesses by adding to the continuing endeavors to work on the quality of EEG signal handling.

2. LITERATURE REVIEW

Akgul, A., Hussain, S., & Pehlivan, I. (2016): This study presents an original tumultuous framework in three aspects that consolidates the cubic, quartic, and quadratic nonlinearities. This clever framework's central dynamical properties, including its fractal aspect, eigenvalue structures, Lyapunov example range, and turbulent ways of behaving, are inspected. Moreover, utilizing a picked boundary, this work investigates the bifurcation examination of the proposed turbulent framework. The turbulent framework has been examined both hypothetically and through broad mathematical investigation. Because of the limitations of electronic parts and materials, plentifulness values assume a huge part in tumultuous frameworks for genuine applications. Subsequently, the new turbulent framework is rescaled and carried out as an electronic circuit for use in a genuine setting. The got results demonstrate that this framework justifies more top to bottom exploration because of its muddled elements and charming highlights. Various logical and designing fields, including physical science, control, cryptology, and random number generators (RNGs), can profit from the new turbulent framework.[1]

Toral, S. L., Martínez-Torres, M. D. R., Barrero, F., Gallardo, S., & Durán, M. J. (2007): An exact exploratory examination concentrate on the utilization of the CMT in the plan of the College of Seville's (Spain) Electronic Engineering (EE) degree is introduced in this paper. Involving the Career-space determinations as a beginning stage, a conceptualizing interaction was utilized to recognize the essential pertinent skills. Utilizing CMT, these skills are organized in view of their proclivity, recognizing and examining the essential groups and their relative importance. To affirm the exactness of the interaction and approve the results for the educational plan adaption, a dependability investigation of the idea maps was at long last led.[2]

Zagirnyak, M., Maliakova, M., & Kalinov, A. (2015): This study talks about the utilization of the small parameter method (SPM) in the recurrence area for the logical assessment of the symphonious parts of flow in electric circuits that contain semiconductor converters. Logical circuit examination involving semiconductor converters in electric circuits was led utilizing a recurrence space SPM. To empower the capability of acknowledgment of calculation in recurrence space, a mechanized method in light of discrete convolution calculation was used to create symmetrical consonant parts of electrical qualities. Utilizing the mathematical estimation method, a semiconductor converter's nonlinear trademark was given. The reference current qualities in the circuit under examination were found utilizing a mathematically organized recreation approach. To make the voltage adjusting conditions in the circuit with a nonlinear component, hypothetical electrical engineering regulations were applied. It is exhibited that applying a SPM and acknowledging it in the recurrence area enormously improves on the scientific examination of electric circuits containing semiconductor converters and makes calculation mechanization more straightforward. The proficiency and adequate exactness of the proposed method were appeared through insightful and mathematical computation of a circuit with a diode under a functioning inductive burden. It is exhibited that rising the number of analyzed music and the request for the approximating polynomial works on the precision of mathematical calculations. Electric devices with nonlinear qualities and electrotechnical devices with semiconductor machines can be determined utilizing the work's outcomes. Besides, the obtained results make it conceivable to explore the methods utilized in electric organizations with a nonlinear burden that contain semiconductor converters to make up for flow higher music.[3]

Bojoi, R., Neacsu, M. G., & Tenconi, A. (2012): An overview of force electronics converter geographies for use in more electric aircraft is introduced in this work, with an accentuation on multi-stage drive frameworks. To improve aircraft effectiveness, reliability, and viability, the airplane business has found that continuously charging on-board benefits is a suitable method for limiting or taking out the need of pressure driven, mechanical, and bleed air/pneumatic frameworks. Electromechanical and electrohydraulic actuators are being presented as a component of an idea known as the More Electric Aircraft (MEA). Moreover, there is a pattern toward leaving consistent recurrence AC energy conveyance for variable recurrence or DC arrangements, and that implies that the whole electrical age and dissemination framework is available to emotional correction. Not many articles gave a review investigation of the power electronic converters utilized in plane applications, in spite of the writing revealing overview papers about electrical machines and their electromechanical plan for the MEA.[4]

3. STATIONARY WAVELET TRANSFORM

Shift variant is a potential issue with DWT that can lead to significant variances in the energy distribution at various scales, significant changes in the reconstructed waveforms, and tiny shifts in the input waveform that result in bigger changes within the wavelet coefficients.

The usual DWT shift variation is made by decimation following filtering. To overcome it, use the Stationary Wavelet Transform (SWT) to remove the decimation after filtering. Thus, without decimation, SWT shares structural similarities with DWT. Since the wavelet coefficients at each level have the same length, the approach is shift invariant.

This study examines the effectiveness of the SWT method for artifact correction using a range of threshold functions and compares it to the DWT technique in terms of common metrics. SWT is briefly described in Section 3.1. Section 4 presents the results and discussions, while Section 5 presents the ultimate conclusions.

3.1. SWT DESCRIPTION

DWT is a very effective tool for many non-stationary signal processing applications since it is non-redundant; nonetheless, it has shift sensitivity, weak directionality, and no phase information.

Numerous academics created real-valued extensions to the conventional DWT, such SWT, to get around these restrictions.

With the exception of the fact that the signal is never sub-sampled in SWT, which is comparable to DWT, every stage of decomposition involves up sampling the filters by adding zeros in between them and limiting the down sampling of decimation.

Since every set of coefficients in the SWT has the same number of samples as the input signal, the technique is inherently redundant. The SWT hierarchy for a two-level sign analysis and synthesis is displayed in Figure 1. For high pass and low pass filters, respectively, use the letters H and L. The High pass and Low pass filters' coefficients, also known as detail and approximation coefficients, are C d and Ca. .

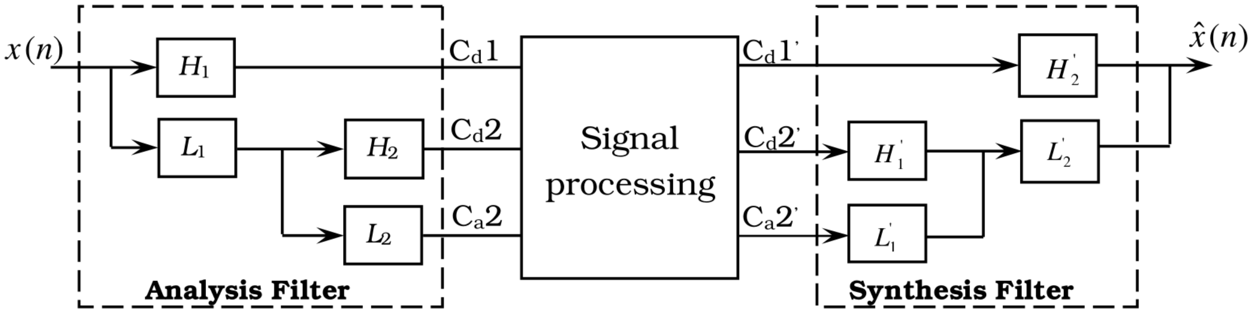

Figure 1: A Two-Level Hierarchy of SWT Denoising

The steps below outline the artifact correction methodology:

(1) SWT breaks down the EEG signal to get the wavelet coefficients for each level. Figure 2 displays the set of detail coefficients for the Fp2 EEG signal.

(2) Determine the signal's statistical measures, including its mean and standard deviation.

(3) After that, a soft thresholding function is used to move the wavelet coefficients to a new location.

(4) Apply the inverse SWT with updated wavelet coefficients to reconstruct the signal.

MATLAB is used for the wavelet decomposition, thresholding, and reconstruction.

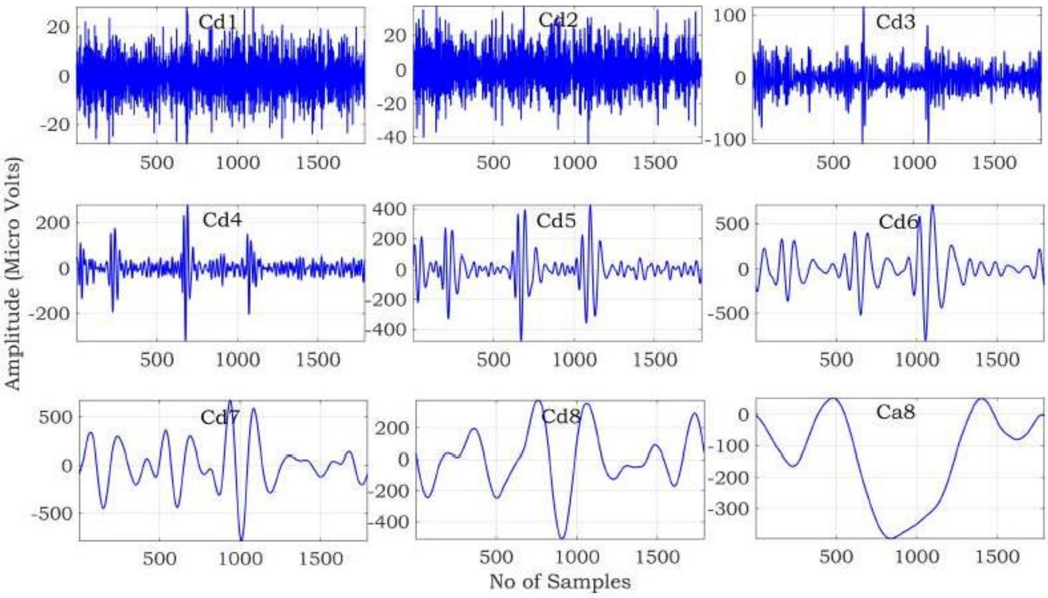

Figure 2: Detail Wavelet Coefficients of Fp2 EEG Signal by SWT

3.2. DETECTION OF SPIKE ZONES

There are several techniques used to identify EEG signal artifacts. When it comes to identifying artifacts, wavelet transform methods have shown to be more successful than temporal or frequency domain approaches. The raw EEG data is divided into 10-second-long epochs, then 'coif5' is used to break down each segment into up to six levels. Each spike typically has three coefficients.

At each level, the approximation coefficients are chosen in the format a j-1, aj, aj+1. The coefficient of variation for each spike zone is computed using the spike zone coefficients (aj-1, aj, aj+1). It is necessary to choose the greater values among the coefficients of variation. This configuration allows for the identification of blinks in the raw EEG output. Figure 3 shows an EEG with the artifacts noted. In the sequel, the rationale behind the division of the artifact zones will be made more evident.

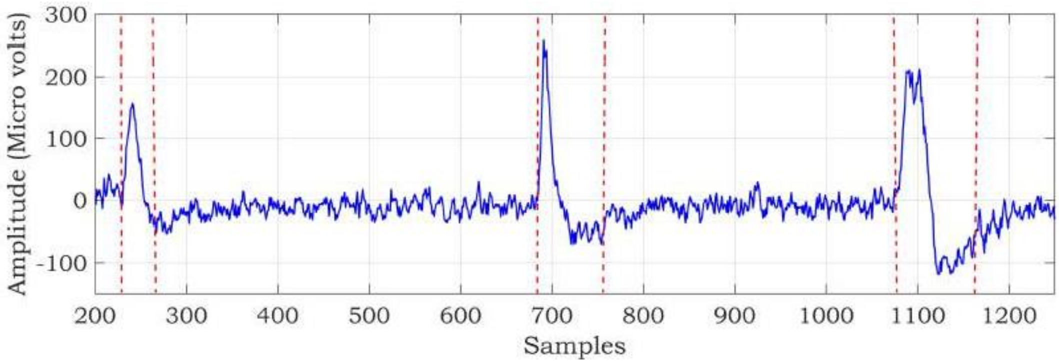

Figure 3: Raw EEG with Identified Artifacts

4. RESULTS AND DISCUSSIONS

This section deals with the correction of OAs from single-channel EEG recordings using SWT with different threshold functions. To demonstrate the effectiveness of the suggested approach, the findings are contrasted with those of the DWT method. Every refined signal's performance indicators, especially ARR and ΔSNR, are assessed and tallied. In the DWT and SWT domains, the effectiveness of artifact removal is primarily reliant on the coefficient thresholding.

4.1. COEFFICIENT THRESHOLDING

The detail coefficients in the DWT and SWT domains before and after thresholding using different threshold functions are shown in Figure 4. Table 1 provides the associated threshold value s for each level in both domains. As an example, the sixth detail coefficient of the Fp2 EEG signal displayed in Figure 2 has been selected.

Detail coefficients prior to thresholding are shown by the blue colored line, and coefficients subsequent to thresholding are represented by the red colored line. Table 1 shows that threshold values via SWT are higher than DWT at every level. Compared to other threshold functions, the NT threshold function has higher values and minimizes the coefficients more effectively.

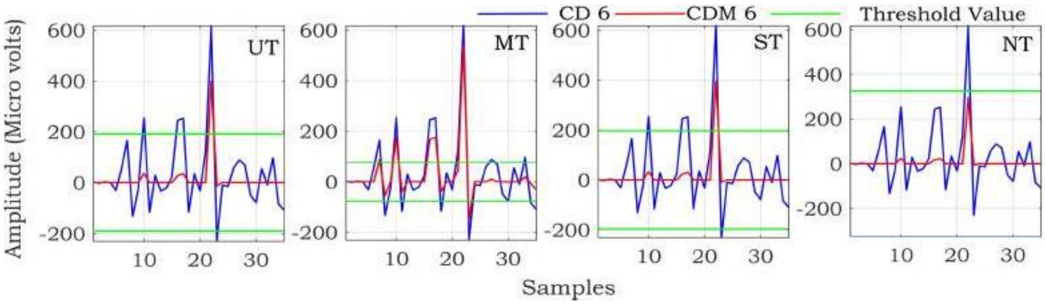

(a)

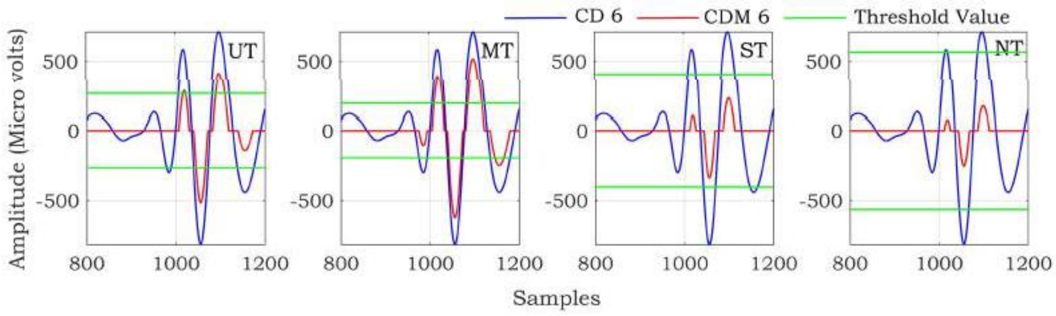

(b)

Figure 4: shows the detail wavelet coefficients using different threshold functions before and after thresholding using (a) DWT (b) SWT

The raw and adjusted EEG signals using WT techniques are shown in Figure 5. The mother wavelet functions "db6" and "db8" are utilized in the DWT and SWT domains, respectively, for the signal decomposition. This figure makes it evident that, for all threshold functions, the SWT approach reduces ocular artifacts more effectively than the DWT method.

The raw and reconstructed EEG signal by SWT employing different threshold functions is shown in Figure 6. SWT+N T and SWT+ST approaches are better at decreasing the artifacts than other combinations. Threshold function NT has demonstrated greater performance than other threshold functions, while ST is the second best at fixing the artifacts. This is because at each decomposition level, NT and ST yield greater threshold values.

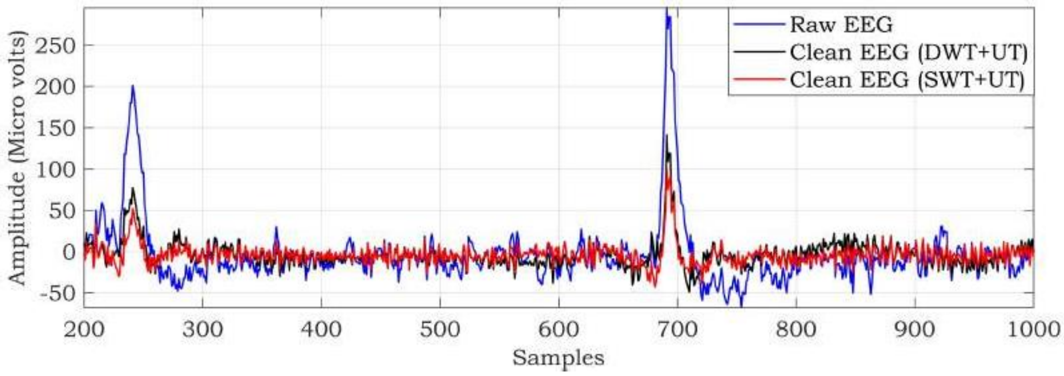

(a)

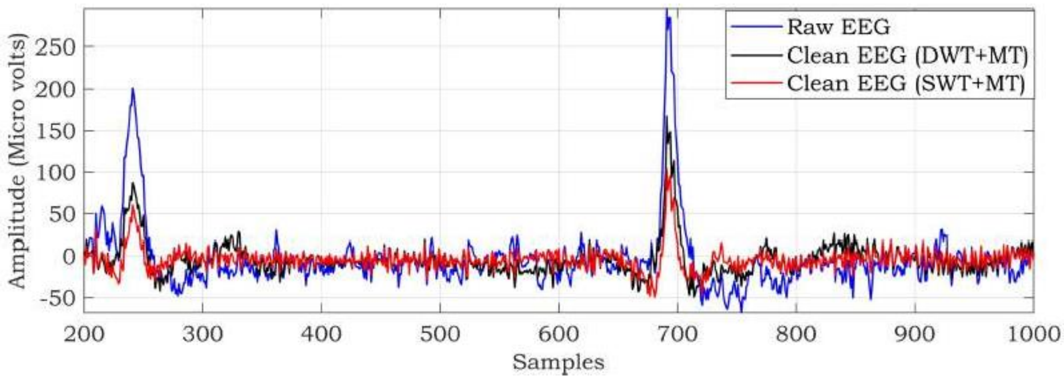

(b)

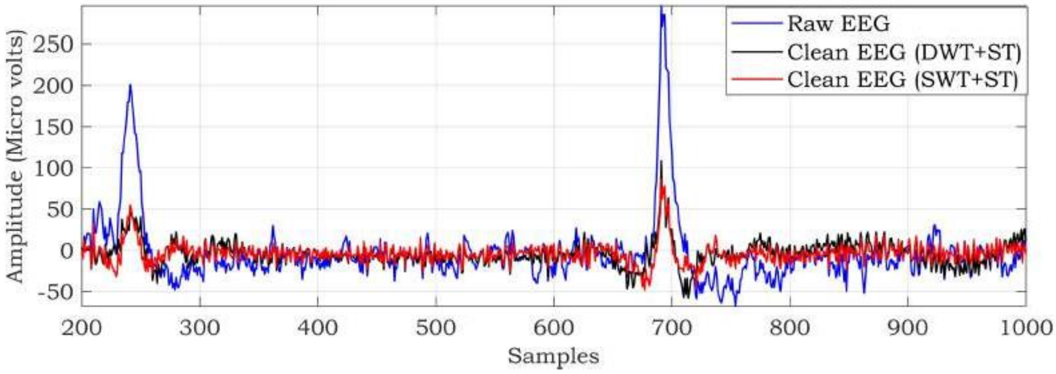

(c)

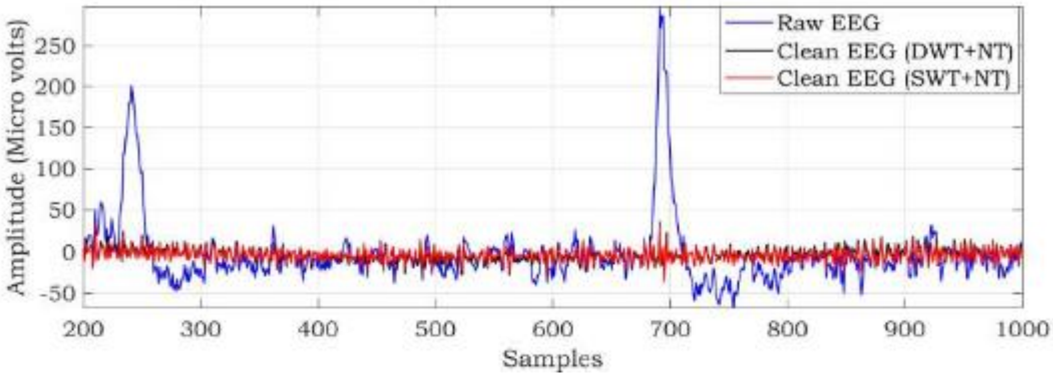

(d)

Figure 5: Raw and Reconstructed EEG Signal s by WT Methods Using Threshold Functions (a) UT, (b) MT, (c) ST, and (d) NT

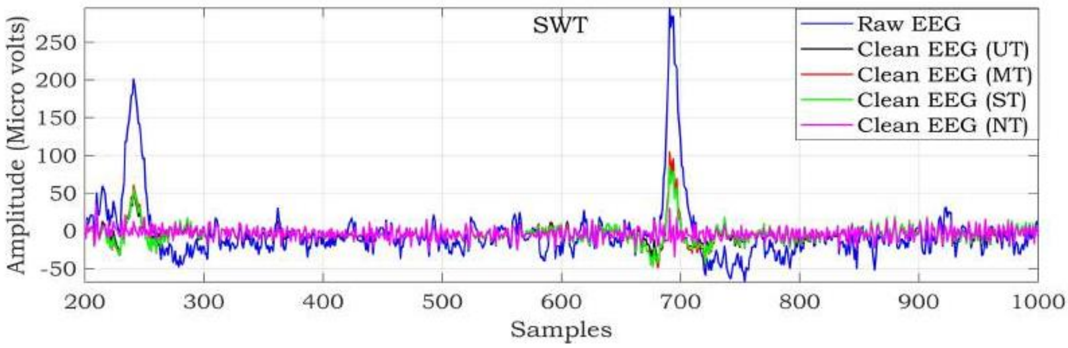

Figure 6: Raw and Clean EEG Signals by SWT using Various Threshold Functions

Figure 7 displays the Power Spectral Density (PSD) of the clean and polluted EEG signals using DWT and SWT methods using different threshold values. These Figures demonstrate that for all threshold functions, SWT reduces the power of the spectral components at lower frequencies more than DWT.

Table 1: Threshold Values of Detail Coefficients Cd5-Cd8 by WT Methods Using Various Thresholds

Method	Threshold Function	Threshold Values of Details C d5-Cd8			
		λ5	λ6	λ7	λ8
	UT	104.0	190.9	290.3	122.7
	MT	51.63	77.34	139.42	27.42

DWT	ST	154.84	196.46	322.89	135.93
	NT	192.56	324.9	628.6	237.86
SWT	UT	143.35	264.30	306.89	214.89
	MT	76.71	193.77	280.54	271.97
	ST	154.14	404.26	589.57	494.54
	NT	174.86	564.30	1148.66	865.44

For all threshold functions, the reconstructed signal at high frequencies is substantially retained in both approaches, suggesting that SWT is a better option than DWT for correcting ocular distortions in EEG recordings.

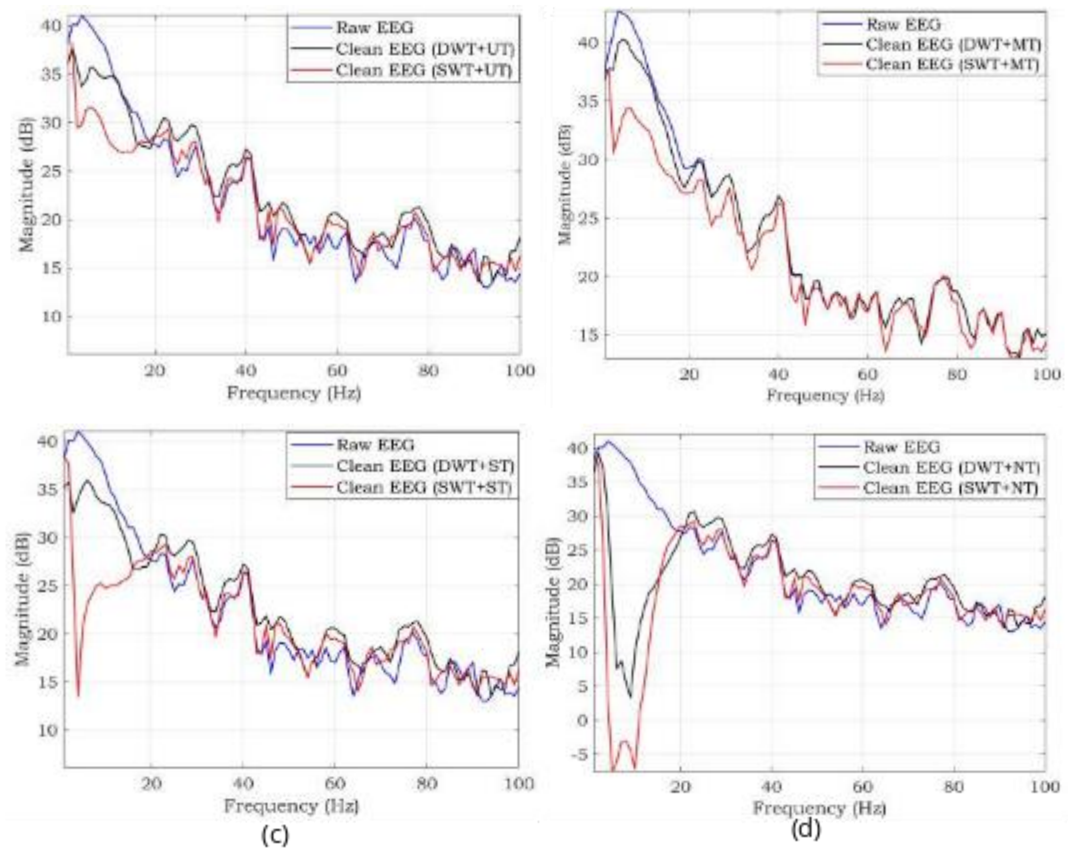

Figure 7: Power Spectra of Original and Clean EEG Signals by WT Methods using Various Threshold s (a) UT, (b) MT, (c) ST, (d) NT

The values of ARR and ΔSNR by SWT employing various wavelet functions are shown in Tables 2–5. Wavelet functions 'db8', 'coif5', and'sym10' exhibit greater ΔSNR and ARR values, suggesting that they are calibrated to the EEG signal under consideration. The zero padding of the filter response at each decomposition level is the reason for the increase in performance metrics by SWT.

Table 2: ΔSNR, ARR for F7 EEG Signal by SWT Using Different Wavelet Functions

Wavelet Functions	Metrics							
	ΔSNR (dB)				ARR			
	UT	MT	ST	NT	UT	MT	ST	NT
db6	10.77	8.85	11.99	12.59	0.95	0.86	1.39	1.56
db7	10.95	9.17	12.14	12.59	1.00	0.89	1.44	1.57
db8	11.12	10.18	12.20	12.59	1.04	0.92	1.46	1.57
coif3	10.19	8.89	11.59	12.59	0.82	0.64	1.24	1.56
coif4	10.36	9.24	11.68	12.59	0.86	0.66	1.29	1.58
coif5	10.48	9.68	11.78	12.59	0.89	0.72	1.33	1.59
sym8	10.32	8.74	11.71	12.59	0.85	0.76	1.30	1.57
sym9	10.47	8.86	11.78	12.59	0.88	0.77	1.31	1.58
sym10	10.45	9.15	11.81	12.59	0.89	0.80	1.34	1.59
bior2.2	9.12	8.04	10.64	12.60	0.58	0.36	0.89	1.43
bior2.4	9.54	8.22	10.99	12.60	0.67	0.54	1.02	1.49
bior2.6	9.72	8.66	11.13	12.60	0.71	0.62	1.08	1.52
rbio2.2	8.97	7.85	10.38	12.60	0.61	0.52	0.94	1.43
rbio2.4	9.50	8.26	11.07	12.60	0.69	0.58	1.10	1.49
rbio2.6	9.76	8.64	11.38	12.60	0.75	0.64	1.20	1.52

Table 3: ΔSNR, ARR for F 8 EEG Signal by SWT Using Different Wavelet Functions

Wavelet Functions	Metrics							
	ΔSNR (dB)				ARR			
	UT	MT	ST	NT	UT	MT	ST	NT
db6	9.16	6.82	11.01	12.23	0.89	0.48	1.56	2.28
db7	9.33	7.22	11.21	12.21	0.93	0.52	1.64	2.28
db8	9.47	7.46	11.45	12.19	0.96	0.56	1.76	2.29
coif3	8.53	6.42	9.86	12.22	0.77	0.52	1.18	2.28
coif4	8.67	6.56	10.04	12.18	0.81	0.58	1.25	2.29
coif5	8.76	6.58	10.21	12.16	0.84	0.60	1.32	2.30

sym8	8.68	6.42	10.05	12.19	0.81	0.58	1.26	2.29
sym9	8.64	6.22	10.22	12.18	0.81	0.57	1.30	2.29
sym10	8.79	6.68	10.21	12.17	0.84	0.59	1.32	2.30
bior2.2	7.79	5.94	9.39	12.38	0.56	0.33	0.90	2.13
bior2.4	8.05	6.02	9.57	12.33	0.63	0.48	0.99	2.21
bior2.6	8.19	6.08	9.71	12.28	0.67	0.48	1.06	2.25
rbio2.2	7.58	5.88	8.69	12.38	0.60	0.44	0.86	2.13
rbio2.4	7.87	5.98	9.33	12.33	0.66	0.46	1.05	2.21
rbio2.6	8.02	6.14	9.56	12.28	0.70	0.52	1.12	2.25

Table 4: ΔSNR, ARR for Fp1 EEG Signal by SWT Using Different Wavelet Functions

Wavelet Functions	**Metrics**							
	ΔSNR (dB)				**ARR**			
	UT	**MT**	**ST**	**NT**	**UT**	**MT**	**ST**	**NT**
db6	11.33	7.82	13.11	16.22	1.21	0.56	1.91	3.60
db7	11.66	8.10	13.70	16.20	1.31	0.59	2.16	3.62
db8	11.95	8.24	14.08	16.19	1.39	0.62	2.35	3.63
coif3	10.16	7.54	10.57	16.21	0.93	0.48	1.08	3.61
coif4	10.40	7.62	11.18	16.18	0.99	0.49	1.25	3.63
coif5	10.58	7.66	11.71	16.16	1.04	0.54	1.40	3.64
sym8	10.35	7.58	10.92	16.19	0.98	0.48	1.18	3.63
sym9	10.52	7.61	11.18	16.18	1.03	0.52	1.28	3.63
sym10	10.55	7.62	11.60	16.17	1.03	0.52	1.38	3.64
bior2.2	8.76	6.68	8.53	16.29	0.60	0.25	0.56	3.33
bior2.4	9.23	7.12	9.12	16.26	0.70	0.34	0.69	3.49
bior2.6	9.46	7.35	9.51	16.26	0.76	0.36	0.80	3.55
rbio2.2	8.44	6.85	8.14	16.28	0.63	0.28	0.63	3.33
rbio2.4	9.11	7.08	9.21	16.26	0.75	0.33	0.84	3.49
rbio2.6	9.44	7.26	10.18	16.26	0.81	0.39	1.07	3.55

Table 5: ΔSNR, ARR for Fp2 EEG Signal by SWT Using Different Wavelet Functions

Wavelet Functions	Metrics							
	ΔSNR (dB)				ARR			
	UT	MT	ST	NT	UT	MT	ST	NT
db6	11.49	8.28	13.41	15.73	1.41	0.67	2.34	3.97
db7	11.79	8.52	13.89	15.70	1.52	0.71	2.63	3.98
db8	12.06	8.80	14.35	15.69	1.62	0.79	2.89	3.98
coif3	10.41	7.67	10.77	15.72	1.10	0.45	1.27	3.97
coif4	10.63	7.84	11.50	15.68	1.17	0.55	1.52	3.99
coif5	10.79	7.98	12.00	15.65	1.23	0.61	1.71	3.99
sym8	10.57	7.74	11.33	15.69	1.15	0.58	1.46	3.98
sym9	10.77	7.86	11.63	15.67	1.23	0.62	1.61	3.99
sym10	10.75	7.92	11.98	15.66	1.21	0.64	1.71	3.99
bior2.2	9.06	6.88	8.70	15.86	0.70	0.25	0.63	3.72
bior2.4	9.54	6.91	9.35	15.84	0.83	0.36	0.81	3.87
bior2.6	9.75	7.02	9.74	15.80	0.90	0.48	0.94	3.93
rbio2.2	8.75	6.45	8.57	15.86	0.74	0.33	0.78	3.72
rbio2.4	9.45	6.98	9.73	15.84	0.88	0.39	1.06	3.87
rbio2.6	9.77	7.15	10.61	15.79	0.97	0.46	1.33	3.93

While threshold function NT consistently provides the best values of ΔSNR and ARR for all wavelet functions, threshold functions UT, MT, and ST with combinations of 'db8' and 'rbio2.2' produce the best and least values of ΔSNR and ARR, respectively. Among all the wavelet functions, threshold function MT provides the lowest values of ΔSNR and ARR.

The performance comparison of WT techniques using the combination of ideal wavelet functions ('db6' and 'db8') for the Fp2 EEG data is shown in Figure 4.8. When it comes to ΔSNR and ARR, threshold function NT performs significantly better than other threshold functions in both approaches. The percentage change in metrics improvement between the proposed approach and a current method is determined using Eq. (1).

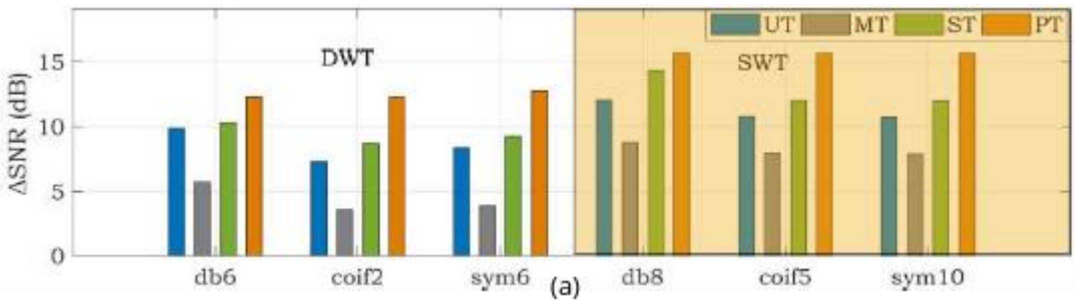

(a)

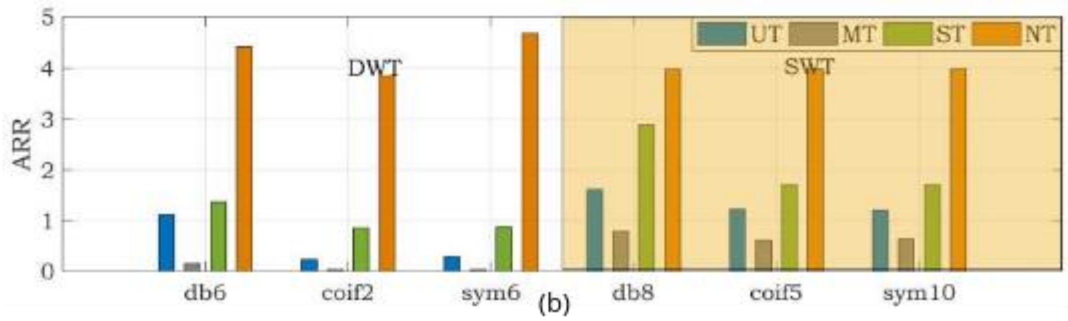

Figure 8: Comparison of Wavelet Functions in DWT and SWT Domains for Fp2 EEG signal by (a) ΔSNR, (b) ARR

Table 5 shows that the improvement in ΔSNR and ARR by SWT+db8+NT compared to SWT+db8+ST is 9.3 and 37.71 percent, respectively. Using Matlab scripts, these methods are run on a Core i9 processor running Windows 11 with 32 GB of RAM. For the same length of data, the average processing times for the two approaches are determined, and the results are given in Table 4.6. This table unequivocally shows that DWT is faster than SWT method; this is because SWT adds a significant amount of redundancy during the signal decomposition process.

Table 6: Average Execution Time of WT Methods

Method	DWT	SWT
Average Execution Time (sec)	0.015	0.05

4.2. RESULTS ON EXPERIMENTAL DATA

The SWT approach is applied to experimental data, just like DWT. Using an ideal wavelet function in both ways, the raw EEG signals are broken down into approximate and detail coefficients. Soft thresholding is then used for details between 5 and 8, and the inverse wavelet transform is used to reconstruct the signal. Figures 9 and 10 show the simulation results in the time and frequency domains before and after the artifact removal. Table 7 presents the average performance metrics of both approaches using different thresholds for the raw and clean EEG signals.

Upon examining Figures 9 and 10, it is evident that the DWT and SWT approaches, which employ different threshold functions, perform better at eliminating artifacts with smaller amplitudes but fall short in minimizing those with larger amplitudes. The power spectra of clean and raw EEG signals obtained by SWT employing different threshold functions are shown in Figure 11.

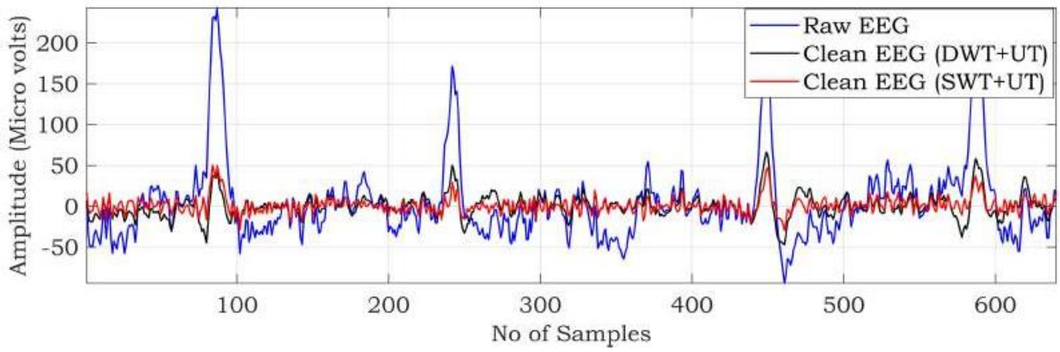

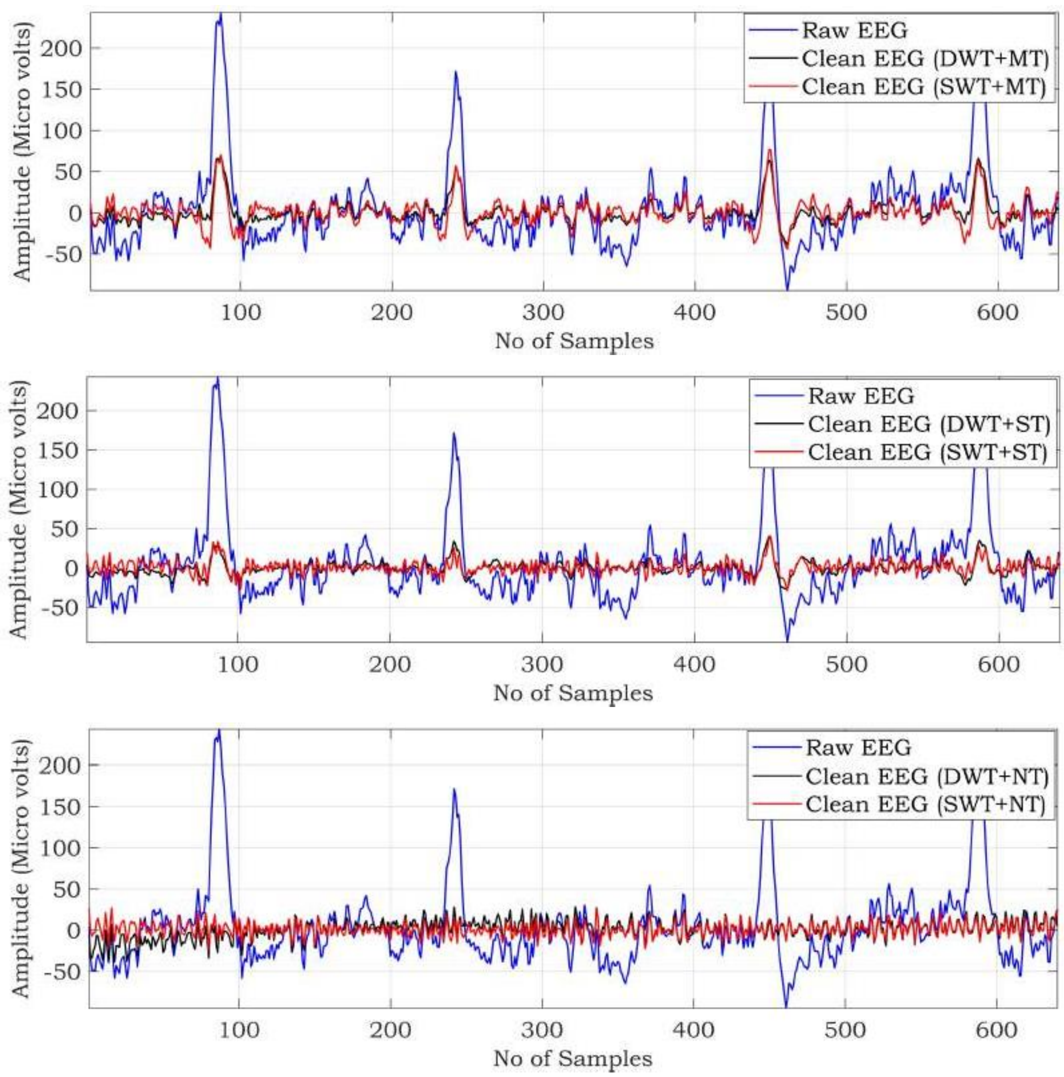

Figure 9: Comparison of EEG Epochs (Multiple Eye Blinks) Before and After Denoising by WT Methods Using Threshold Functions (a) UT, (b) MT, (c) ST, (d) NT

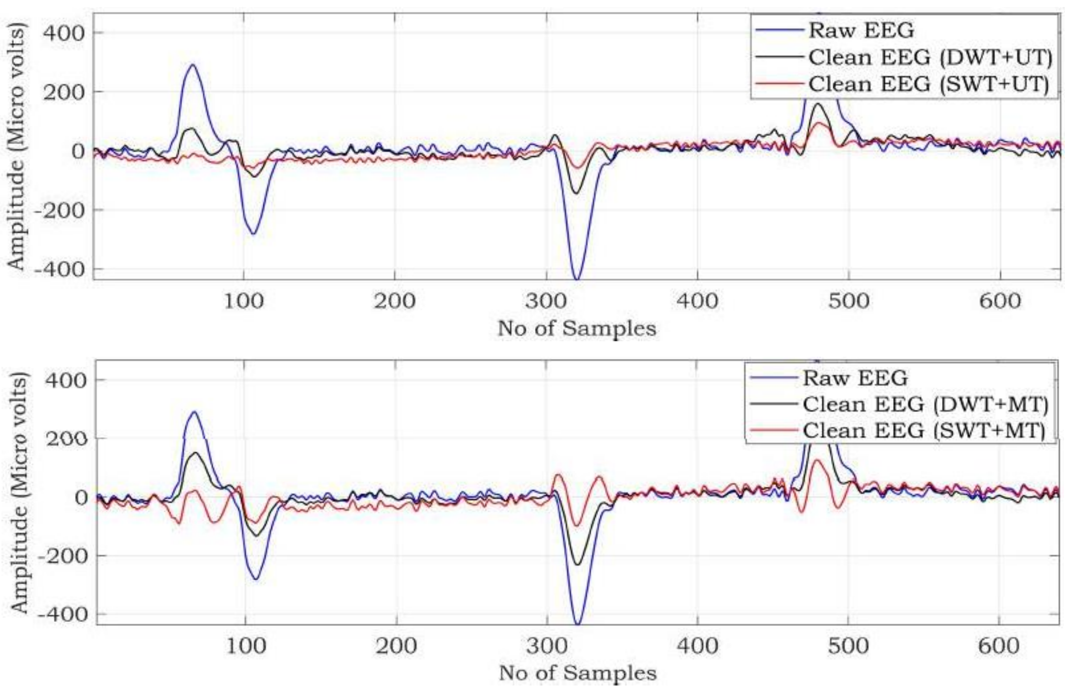

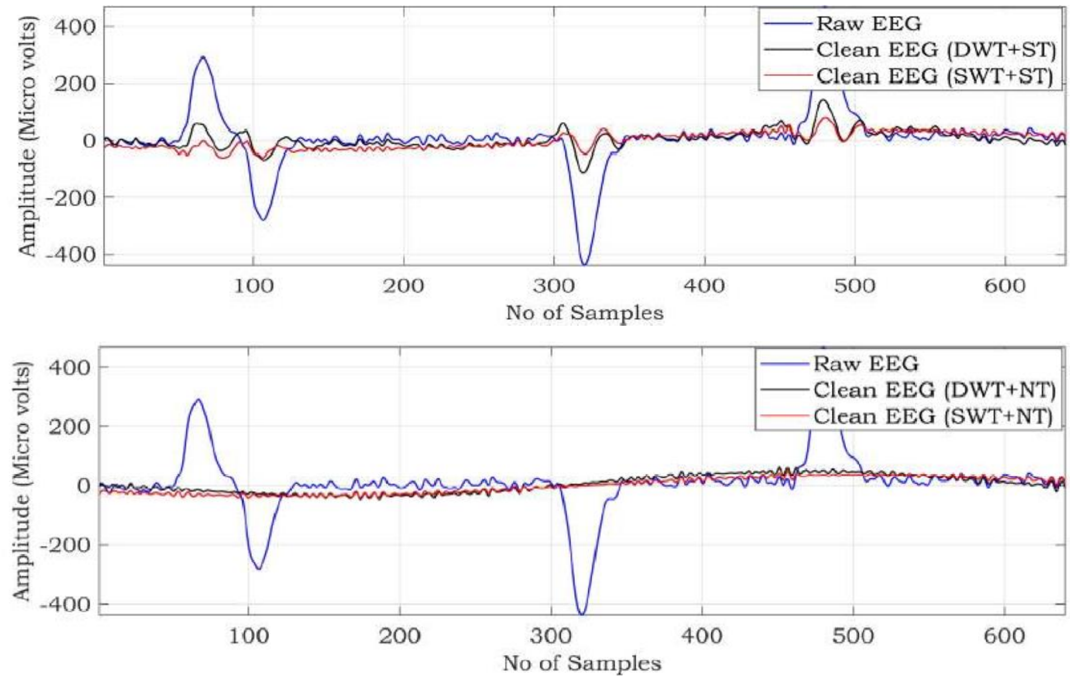

Figure 10: Comparison of EEG Epochs (Large Eye Blinks) Before and After Denoising by WT Methods Using Threshold Functions (a) UT, (b) MT, (c) ST, (d) NT

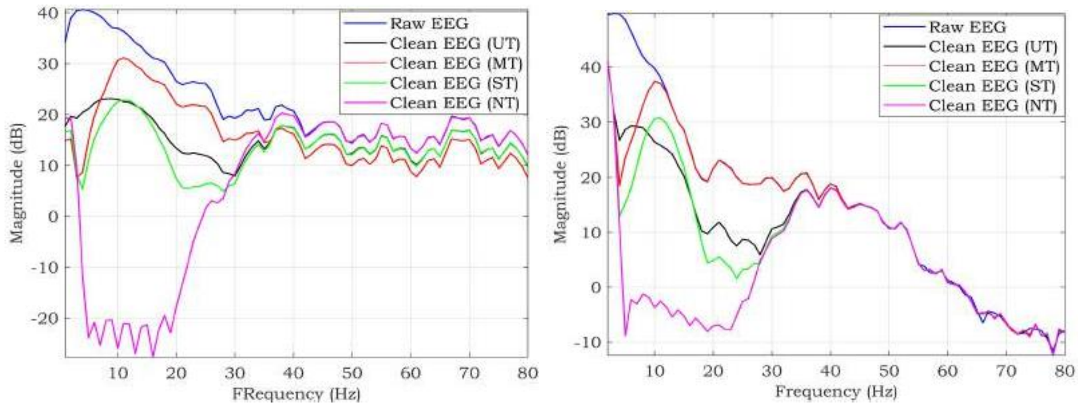

Figure 11: Clean and Contaminated EEG Signal Power Spectra by SWT Using Different Threshold Functions (a) Blinks from several eyes (b) Blinks from larger eyes

While threshold function NT reduces artifacts more effectively than other threshold functions, over non-blink regions the reconstructed signal produced by NT differs from the actual EEG signal.

Table 7: Average ΔSNR and ARR Using Different Threshold Functions for WT Methods Comparing Raw and Clean EEG Signals

Methods	Thresholds	Metrics	
		ΔSNR	ARR
DWT	UT	10.82	2.14
	MT	7.54	1.22
	ST	12.24	3.26
	NT	16.18	4.28
	UT	19.45	8.86

SWT	MT	12.66	4.48
	ST	22.88	12.92
	NT	24.24	16.26

The background data in non-artifact regions should be preserved while the artifacts in the blink zone are eliminated using an efficient artifact removal technique. The EEG signal is divided between regions that blink and those that do not, and the raw and reconstructed EEG signals at n on-blink regions are compared for Correlation Coefficient (CC) and Root Mean Square Error (RMSE). The Fp2 EEG signal's CC and RMSE values obtained using various techniques are shown in Table 8.

Table 8: CC and RMSE between Raw and Clean Fp2 EEG Signals by WT Methods

Method	**Threshold**	**Metrics**	
		CC	**RMSE**
DWT	UT	0.955	14.94
	MT	0.972	13.07
	ST	0.742	16.85
	NT	0.473	21.24
SWT	UT	0.968	11.08
	MT	0.990	9.69
	ST	0.782	14.77
	NT	0.559	18.75

CC is a statistical quantity that shows the degree of similarity between two signals given by Eq. (2).

$$CC = \frac{\sum_{n=1}^{N}(X_1[n] - \overline{X_1})(y_1[n] - \overline{y_1})}{\sqrt{\sum_{n=1}^{N}(X_1[n] - \overline{X_1})^2 \sum_{n=1}^{N}(y_1[n] - \bar{y}_1)^2}}$$

RMSE estimates the difference bet ween the raw and clean EEG data given by Eq. 3

$$RMSE = \sqrt{\frac{1}{N}\sum_{n}(X_1[n] - y_1[n])^2}$$

Where x 1[n] and y1[n] represents the raw and reconstructed EEG signals in artifact free regions.

Table 8 shows that while NT produced poor outcomes in both techniques, MT and UT performed better based on the CC and RMSE threshold functions. At every decomposition level, the exponential threshold improvement factor of NT could be the cause.

5. CONCLUSION

This work proposes OA correction in single-channel EEG using SWT utilizing different thresholds. The effectiveness of the suggested approach is contrasted with the current method (DWT) using the following metrics: power spectrum, ΔSNR, ARR, CC, and RMSE. It is noted that the threshold function NT produced a better result than other thresholds in terms of ΔSNR and ARR, and that the SWT approach performed better than the DWT method. But in terms of CC and RMSE, threshold functions UT and MT have performed better than other thresholds. While threshold function NT does a better job of rejecting artifacts, it still has to be improved because it significantly affects the neural information in non-blink regions. On the other hand, SWT requires more processing and redundancy. Additionally, wavelet transform (SWT, DWT) lacks adaptability. The performance of artifact removal is also affected by the wavelet that is chosen.

REFERENCES

1. Akgul, A., Hussain, S., & Pehlivan, I. (2016). A new three-dimensional chaotic system, its dynamical analysis and electronic circuit applications. *Optik*, *127*(18), 7062-7071.
2. Toral, S. L., Martínez-Torres, M. D. R., Barrero, F., Gallardo, S., & Durán, M. J. (2007). An electronic engineering curriculum design based on concept-mapping techniques. *International Journal of Technology and Design Education*, *17*, 341-356.
3. Zagirnyak, M., Maliakova, M., & Kalinov, A. (2015). Analysis of electric circuits with semiconductor converters with the use of a small parameter method in frequency domain. *COMPEL: The international journal for computation and mathematics in electrical and electronic engineering*, *34*(3), 808-823.
4. Bojoi, R., Neacsu, M. G., & Tenconi, A. (2012, June). Analysis and survey of multi-phase power electronic converter topologies for the more electric aircraft applications. In *International Symposium on Power Electronics Power Electronics, Electrical Drives, Automation and Motion* (pp. 440-445). IEEE.
5. Acharya, U. R., Joseph, P. K., Kannathal, N., Min, L. C., and Suri, J. S., Heart rate Variability: a review. Med. Biol. Eng. Comput. 44(12):1031–1051, 2006 doi:10.1007/s11517-006-0119-0.
6. Akaike, H., Fitting autoregressive models for prediction. Ann. Inst. Stat. Math. 21:243–247, 1969 doi:10.1007/BF02532251.
7. Bai, D., and Li Qiu, T., The sample entropy and its application in EEG based epilepsy detection. J. Biomed. Eng. 24(1):200–205, 2007.
8. Bhattacharya, J., and Petsche, H., Phase synchrony analysis of EEG during music perception reveals changes in functional connectivity due to musical expertise. Signal processing. 85 (11):2161–2177, 2005 doi:10.1016/j.sigpro.2005.07.007.
9. Bruhn, J., and Ropcke, H., Approximate entropy as an electroencephalographic measure of anesthetic drug effect during desflurane anesthesia.. Anesthesilogy. 92(3):715–726, 2000 doi:10.1097/ 00000542-200003000-00016.
10. Bullock, T. H., Achimowicz, J. Z., Duckrow, R. B., Spencer, S. S., and Iragui-Madoz, V. J., Bicoherence of intracranial EEG in sleep, wakefulness and seizures. Electroencephalogr. Clin. Neurophysiol. 103:661–678, 1997 doi:10.1016/S0013-4694(97) 00087-4.
11. Dias-Tosta, E., Kuckeihaus, G. S., Amaral, K., Sinha, J., Kurup, A., Paleti, A., et al., Decrease of non-linear structure in the EEG of Alzheimer patients compared to healthy controls. Clin. Neurophysiol. 110(7):1159–1167, 1999 doi:10.1016/S1388-2457(99) 00013-9.
12. Ding, M., Grebogi, E., Ott, E., Sauer, T., and Yorke, J. A., Estimating correlation dimension from a chaotic time series:when a plateau occurs? Physica. D. 69:404–424, 1993 doi:10.1016/ 0167-2789(93)90103-8.
13. Fell, J., and Roschke, J., A Comparison between spectral and nonlinear EEG measures. Electroencephalogr. Clin. Neurophysiol. 98(5):401–410, 1996 doi:10.1016/0013-4694(96)95636-9.

14. Fraser, A. M., and Swinney, H. L., Independent coordinates for strange attractors from mutual information. Phys. Rev. A 33:1134– 1140, 1986 doi:10.1103/PhysRevA.33.1134

15. Gigola, S., Ortiz, F., D'Attellis, C. E., Silva, W., and Kochen, S., Prediction of epileptic seizures using accumulated energy in a multiresolution framework. J. Neurosci. Methods. 138(1–2):107– 111, 2004 doi:10.1016/j.jneumeth.2004.03.016.